Contactless temperature monitoring of the back surface of a woven-ply laminate under fire exposure

Tanguy Davin, Lanhui Lin, Julie Vacandare, Fabrice Barbe, Mouldi Ben Azzouna, Benoit Vieille

CONTACTLESS TEMPERATURE MONITORING OF THE BACK SURFACE OF A WOVEN-PLY LAMINATE UNDER FIRE EXPOSURE

Tanguy Davin[1], Lanhui Lin[1], Julie Vacandare[1], Fabrice Barbe[1], Mouldi Ben Azzouna[1], Benoit Vieille[1]

[1]Groupe de Physique des Matériaux (UMR CNRS 6634), INSA Rouen Normandie, Univ Rouen Normandie, 76801 St Etienne du Rouvray, France

http://www.insa-rouen.fr and http://gpm.univ-rouen.fr

tanguy.davin@insa-rouen.fr, lanhui.lin@insa-rouen.fr, julie.vacandare@insa-rouen.fr
mouldi.ben-azzouna@insa-rouen.fr, fabrice.barbe@insa-rouen.fr, benoit.vieille@insa-rouen.fr

Keywords: IR thermography, Fire degradation, Changing emitting surface, Heat transfer conditions, Parameters identification

Abstract
Fire exposure conditions that are used to reproduce fire events in aircrafts engine are considered in this study. In order to characterize the heat transfer involved in a composite material subjected to a kerosene flame, the boundary conditions of the thermal problem are analyzed. The heat transfer representation are described as well as several methods to characterize the heat fluxes.
An experimental kerosene burner is employed to mimic the fire certification conditions (flame temperature of 1100 °C and heat flux of 116 kW/m² around the impinging zone) and an infrared camera is used to monitor the back surface temperature of a sample. As first step towards a characterization of the measurement set-up, a steel plate is used on these conditions, the heat fluxes are quantified in a wide area, on either back surface (global convective coefficient) or exposed surface (local radiative and convective heat fluxes).

1. Introduction

Composites materials are widely used for the lightening of structures for transport parts because of their high specific properties. For aeronautics applications, an important issue is the fire resistance [1]. Thermoplastic composites have shown a very high degree of mechanical performance under severe environmental conditions (high temperature or flame exposure) [2-3]. But better understanding and control of their mechanical behavior evolution under a localized severe thermal aggression requires an accurate knowledge of the thermal fields, both through the thickness and within the laminate planes. It is thus particularly important, in this framework of the thermo-mechanical characterization, to correctly represent these heat transfer conditions. This study focuses on two objectives: (Obj1) analyzing the available temperature measurements techniques and (Obj2) properly representing the heat transfer conditions under one-side fire exposure.

Critical service conditions as flame exposure possibly combined with mechanical loading induce difficulties to achieve robust temperature measurements (Obj1). Sticking probes such as thermocouples is not trivial. Also they are punctual and intrusive. Two contactless techniques are promising to determine the 2D surface temperature. With thermal coating referring to as Thermographic Phosphors or Temperature-Sensitive Paintings [4-5], the temperature signal can be extracted from the radiation disturbance on the exposed surface but the method is complex and remains slightly intrusive. IR thermography, though the exposed surface cannot be visualized due to the lack of emission signal compared to flame's, can be implemented on the back surface. Measurements on the exposed surface

remains a challenge: the higher intensity of the flame's emission signal as compared to that of the exposed surface itself makes IR thermography unsuitable. Phosphor thermometry then seems to be the only potential solution. But again, its intrusive aspect raises questions on the potential effects of this technique on the flame-material interactions and the melting and decomposition mechanisms of the thermoplastic matrix [5].

In the present study, IR thermography was considered to assess the back temperature in order to investigate the heat transfer conditions. The determination of the temperature from IR signal emission, in severe or critical service conditions, raises two issues: the intrinsic heterogeneity of the emission of the composite sample, and its emissivity with respect to the temperature. The surface state might change due to its thermal decomposition during the test, in terms of aspect in terms of aspect (transition states of the matrix [6]) and geometry (swelling)[7].

The assessment of the heat transfer boundary conditions (Obj2) must be based on a heat transfer model from which parameters, namely the emissivity and convection coefficients, can be identified as was previously proposed [8]. However, the studied composite material of interest comprises many thermophysical properties uncertainties due to heterogeneity of the mesostructure: surface and volume heterogeneity respectively influences emissivity and conductivity. These biases cause perturbation in the representation of the heat transfers. Experimentally, the identification technique on a representative isotropic material without any heterogeneous mesostructure (either surfacic) is then considered in order to characterize the boundary conditions of a sample exposed to the kerosene flame. This identification method will firstly consist in monitoring the sample temperature homogeneity during heating to adapt the degree of thermal representation. The chosen isotropic thin metallic plate is a highly conductive material enabling to rely on simplifying assumptions for the representation of the heat transfers. The homogeneous heat flux of the kerosene-flame (previously quantified [9-11]) is considered to identify the back surface convection.

2. Experimental set-up and methodology

2.1. Material and experimental set-up

An apparatus is used to reproduce the local accident conditions of standards in aeronautics (also employed during thermo-mechanical tests). This bench is based on a domestic burner supplied by Cuenod: it is composed of a kerosene nozzle producing a 80° hollow cone spray conveyed in a 50 mm diameter tube. The air and kerosene supplies are controlled to guarantee a 0.3 g/s kerosene flow rate and an air/fuel mixture at 0.85 of the stoichiometric value. These conditions produce a flame temperature of 1100°C and a heat flux of 116 kW/m² at the impinging zone. A protective shield is placed between the sample and the flame outlet. This 10 mm insulating shield limits the area affected by the flame to an area of 170x130mm². During the fire aggresion, a Long-Wave InfraRed (LWIR, 7.5-14µm) camera, A655sc supplied by FLIR, is employed to measure the 2D temperature field of the back surface. Figure 1 gives an overview of the experimental set-up whereas Figure 2 reprents a schematic view of the zone of interest.

The woven-ply composite laminates present heterogeneity in structural and thermophysical properties. The resulting anisotropic bulk properties can be assessed but they present bias. Also, as the bulk thermal conductivity is of several times superior in the in-plane direction than through the thickness, the measurements done alongside with this study on such composites subjected to fire show a relatively homogeneous 2D temperature field within the exposed area, which would make the characterization less reliable. In addition, the degradation of a composite material when exposed to the flame implies degradation effects, that present endo or exo-thermal transformation, and changes in both geometrical and in composition. As the flame exposure induces many uncertainties on the thermal conditions, a material with known thermo-physical properties is employed to be exposed to the flame. A 201x170x1 mm 304L laminated stainless steel plate was chosen as this representing sample without any phase transformation. This metallic plate is physically stable when exposed to a flame. However, it presents an important reflectance (mirror effect inducing disturbing radiations) and a propensity for

oxidation which highly modifies the emission. The plate was then coated on both sides with a high-temperature-resistant black painting. Table 1 gives the used thermo-physical properties of the steel at room temperature. They are considered temperature-independent and the conductivity is given for the thermally thin assumption purpose.
For these painted surfaces, an emissivity of 0.95 is assumed. Also, as the whole plate was not observable normally to the back surface with the camera (hot environment), an oblique viewpoint was used (see left hand side of Figure 1). The monitored images data were adapted to consider both the radiation theory and geometrical distortion. First, a Lambertian emission with a constant 35° angle from the back surface normal was assumed to correct the spatial distribution of the emission. Then a linear interpolation was adopted to twist back the image for a rectangular representation (Figure 3).

Table 1. Thermo-physical properties of 304L SS

Specific heat capacity (c_p)	Density (ρ)	Thermal conductivity (k)
510 J/(kg.K)	7955 kg/m^3	16 W/(m.K)

Figure 1. Experimental fire bench: direct oblique view on steel plate (left) and normal reflected view on a composite laminates (right) subjected to a kerosene flame

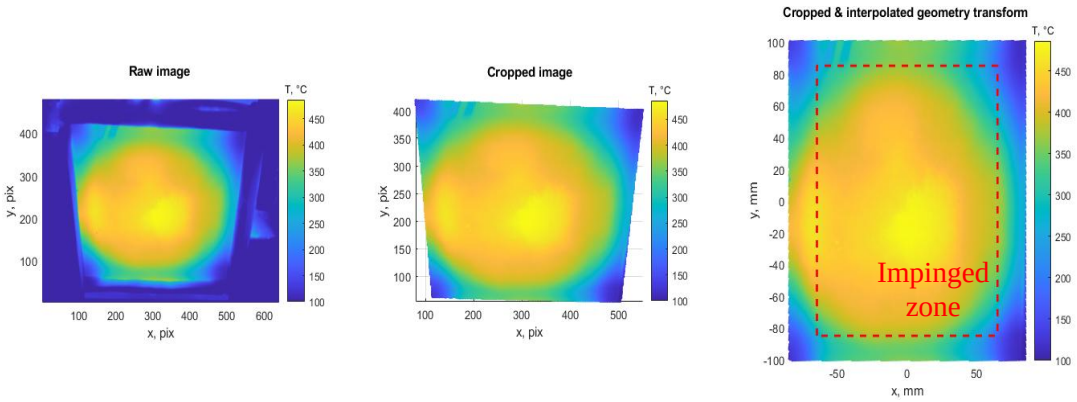

Figure 2. Geometrical image processing: raw temperature image (left); sample plate cropped (middle); geometry transformed (right)

2.2. Heat transfer considerations

The external heat fluxes resulting from a kerosene flame exposure on the exposed surface and from

natural convection on the back surface are schematized in Figure 3: the surfaces exchange heat through radiation and convection. Internal heat transfer i.e. conduction is not represented as simplifying assumptions can be done as described later in this part. The radiative and convective heat fluxes on a sample surface can be explicited respectively by the Stefan-Boltzmann and the convection laws.

$$\begin{aligned} \phi^{rad} &= \sigma T_s^4 \\ \phi^{cv} &= h(T_\infty - T_s) \end{aligned} \tag{1}$$

Where σ is the Stefan–Boltzmann constant, h is the convective coefficient, T_∞ and T_s are respectively the fluid core and the sample (s) surface wall temperatures. Here the heat flux is normal to the surface and taken positive if absorbed by the sample. The radiative heat flux ϕ_{rad} is affected by a $-\epsilon$ or $+\alpha$ factor depending if the flux is emitted or absorbed. The total heat flux on the exposed (e) and back (b) surface can thus be expressed as follows:

$$\begin{aligned} \phi_e &= \phi^{rad} + \phi_e^{rad\,em} + \phi_e^{cv} = \alpha_e \phi_e^{rad} - \epsilon_e \sigma T_{s_e}^4 + h_e\left(T_f - T_{s_e}\right) \\ \phi_b &= \phi_b^{amb} + \phi_b^{rad\,em} + \phi_b^{cv} = \alpha_b \sigma T_{amb}^4 - \epsilon_b \sigma T_{s_b}^4 + h_b\left(T_{amb} - T_{s_b}\right) \end{aligned} \tag{2}$$

Where T_f is the flame temperature, and T_{amb} the ambient air above the back surface. ϕ_e^{rad} is the radiative flux of the flame that can be described as a complex contribution of particles, gas and the burner walls radiations [12]. Also, for the radiative part, the realistic assumption of the gray body ($\epsilon \sim \alpha$) can be done.

The conduction within the sample is analyzed and can be expressed by the Fourier's law. In the case of the steel thin plate, the consideration of the Biot number $Bi = \frac{h_e e}{k} \sim 0.003$, e and k as the sample thickness and thermal conductivity, agrees well with a thermally thin behavior (even the total Biot number accounting for the radiative and convective parts relative to the conductive one is about 0.007). The in-plane conduction can also be discussed. The surface 2D temperature field can help assessing the radial conductive flux. The radial conductive heat power through a 50 mm diameter area, calculated from the mean temperature gradient on the whole sample in the steady regime (around 3,000K/m) is about 3% of the axial heat power resulting from the flux ϕ_e received on a 50 mm diameter disc. Radial heat fluxes can then be neglected to a first approximation. Along with the thermally thin assumption, the transient energy balance on an elementary plate surface, considered isothermal and with negligible exchange with adjacent ones, can be expressed as:

$$\phi_e + \phi_b = \phi_{calo} = \rho_s c_p . e \frac{dT_s}{dt} \tag{3}$$

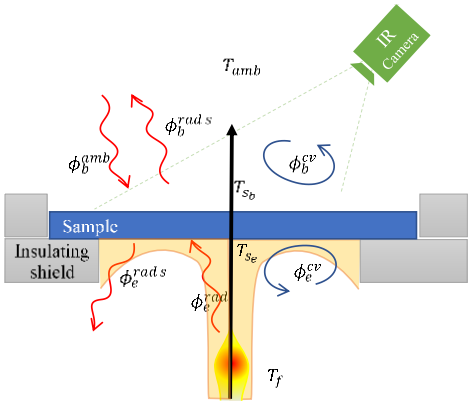

Figure 3. Sketch of a sample under kerosene-flame attack: infrared visualization and interface heat transfer representation

With those thermal considerations, two approaches are proposed to evaluate the heat fluxes on interfaces:

A. Assuming the heat flux on the impinging area of the exposed surface as previously characterized, the global convective coefficient on the back surface h_b is identified. It can be compared to the reference value on natural convection on a horizontal plate.
B. Assuming the global convective coefficient on the back surface h_b , the local heat flux ϕ_e^{flame} on the impinging area of the exposed surface is identified.

The heat flux at the center of the surface impinged by the kerosene-flame in the same conditions were previously quantified by Schuhler et al. [11]. Hence the exposed surface parameters are h_e = 52.5 W/(m².K) and ϕ_e^{rad} = 66 kW/m². This parameter set was chosen to assess the heat flux ϕ_e in the so-called method A. For method B, the two parameters are not decorrelated and only the total ϕ_e is locally determined. For both methods A and B, the combination of Equations (2) and (3) leads to an explicit formulation of all the heat fluxes, especially the convective coefficient on the back surface h_b. For method A, both steady and transient regime are considered whereas here only the steady state is exploited for method B.

3. Results and discussion

Figure 4 shows the temperature measurements obtained from the IR camera measurements on the back surface. The time evolution of the steel plate exposed to the kerosene fire for 250 seconds and the cooling can be seen on the left side. The maximum temperature is reached after 100 seconds. Then, the monitored temperature slightly decreases. That might be due to the formation and growing of a soot layer on the exposed surface, but also the change in radiative surface properties (absorptivity and emissivity). The steady regime is defined as the state at maximum temperature when the conditions are closer to the initial ones. Figure 4b presents the 2D field temperature in the steady regime. A dissymmetry can be observed and is probably due to the deformation of the plate, resulting from the thermal gradients. This curvature alters slightly the geometry and changes the emitting surface normal as observed by the camera. Also, some exhaust gas of the flame jet was observed to pass between the insulating shield and the plate that might explain the hot spot on the left side of the plate.

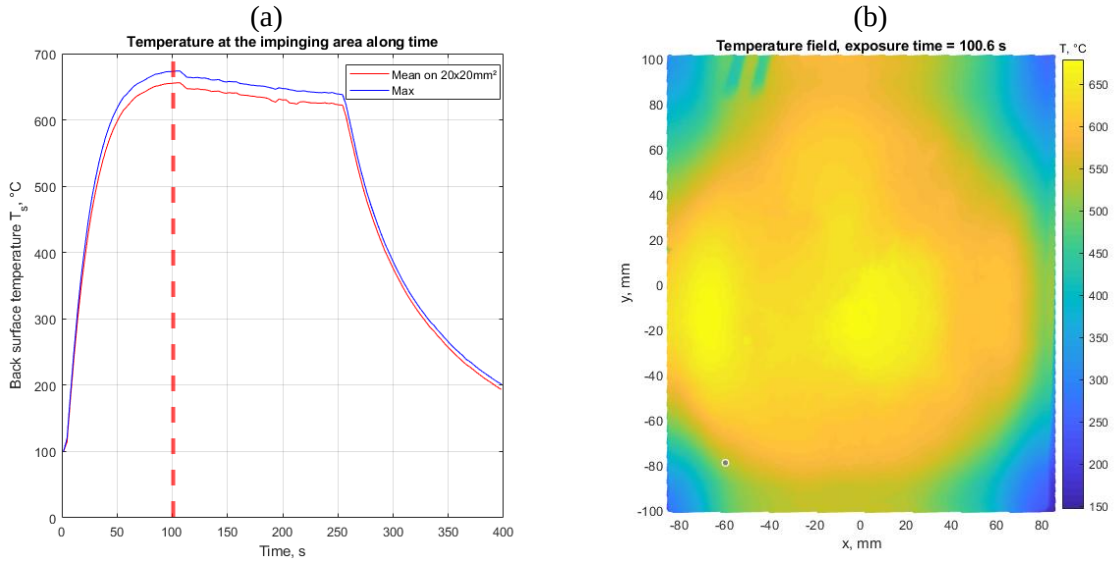

Figure 4. Time evolution of the back surface temperature at the center during the fire exposure and cooling (a) and the temperature field at the thermal steady state (b).

3.1. Convection characterization assuming the center fire conditions (method A)

As a first approach, only the steady state is considered in the center of the plate. A central 20x20 mm² zone is employed to average the temperature representative of the impinging zone. Noteworthy the in-plane conductive heat flux is all the more justified as gradients are limited. At the center, the temperature stabilizes at about 660 °C after a 100 seconds exposure. The heat fluxes on exposed and back surfaces balance, as formulated by Equation (3) with a null right term. Assuming the previously quantified flame heat flux parameters, the convective coefficient on the back surface can be explicitly calculated (method A). A value of 8.1 W/(m²K) is computed. The heat transfer by natural convection on the upper surface of hot plate is addressed in [13]. Depending on the ambient air properties considered at 660°C or at room temperature, the convective coefficient falls between 13.4 and 15.0 W/m²K.

The methodology is extended to the transient regime, and the whole exposure/cooling sequence is considered. The same assumptions on the fire parameters (especially ϕ_e^{rad} and h_e) are done, but the right term in Equation (3), the calorimetric heat flux ϕ_{calo} due to heat accumulation, is no longer neglected. The evolution of the convective coefficient is given in Figure 5b. All the heat fluxes terms are also provided (Figure 5a) to help understanding the energy balance. It is worth noticing that among the other terms, the back surface convection ϕ_b^{cv} is not predominent. Its reasonably low variations during the steady state results in an important change in the convective coefficient. The identified value, which is greatly sensitive to the sample temperature, is thus not very accurate even though the order of magnitude is consistent with literature. Also, the drift in the coefficient might be possibly due to the growing soot layer that should not only change the conductive and radiative interface at the exposed surface, but also provide more insulation by the added conduction in the soot porous layer.

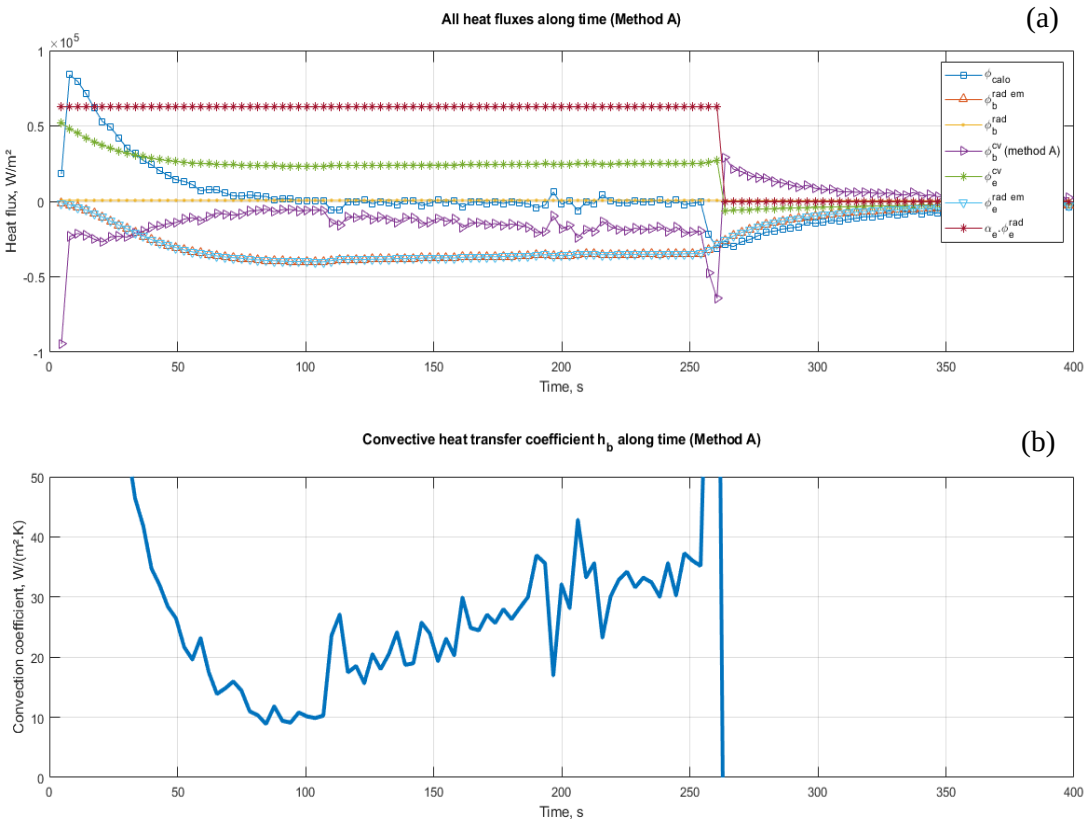

Figure 5. Method A: Time evolution of all the heat fluxes at the center by considering the exposed surface boundary conditions parameters by [11] (a) and the resulting back surface convective coefficient h_b (b)

3.2. Local flux at the exposed surface assuming constant back convection (method B)

The convective coefficient on the back surface is then accounted for constant (the previously identified value at steady state) and the local distribution of the heat flux at the exposed surface is investigated. As the emitted radiative flux of the sample $\phi_e^{rad\ em}$ depends on the impinged surface emissivity and temperature, the flame heat flux ϕ_e^{flame}, which is the sum of the radiative and convective contributions of the flame, is represented as in Figure 6a. The local distribution of ϕ_e^{flame} is also plotted as a profile (Figure 6b) along the radius calculated from the plate center. Though the dissymmetry is still observed, the distribution shows a relatively constant heat flux at the center and a decrease that becomes more and more pronounced moving away from the center.

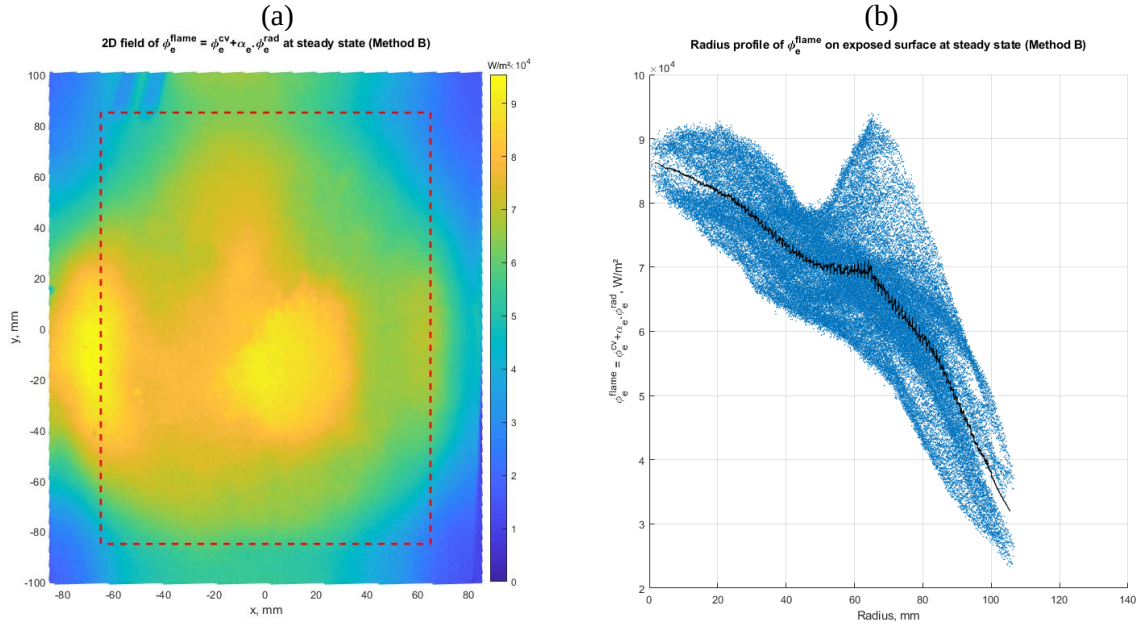

Figure 6. Method B: 2D flame heat flux field ϕ_e^{flame} at steady state after a 100s kerosene flame exposure (a) and the resulting radial profile (b), by considering a constant h_b = 8.1 W/(m²K)

4. Conclusion

The present study aims at a better understanding of the heat transfer involved in composite materials subjected to severe temperature conditions as fire. The present paper shows a dual methodology for the identification of key parameters of the heat transfer intervening in such a thermal attack. The thermal problem presenting numerous uncertainties, the study has focused on an inert material, a steel plate, for sake of simplicity.

The results show a relatively good agreement between the obtained convective coefficient on the back surface and the literature values. Despite dissymmetry, probably due to the optical measurements and the insulation/plate contact conditions, a trend of the flame heat flux distribution is observed. The flame heat flux profile shows a gradual decrease from the center to the sides.

The upcoming work will focus on a better control of the experimental conditions and the analysis of both the soot formation and the sample radiative properties that might disturb the heat flux at the front surface. The values of the identified thermal parameters will then be used as input parameters (boundary conditions) of a direct method, to compare the temperature profiles resulting from the modelling and an experimental case with a thermally thick composite material. Along with the composition analysis, geometry and resulting thermal properties, this work will eventually foster the understanding of the complex thermo-mechanical behavior of composite materials subjected to critical service conditions.

References

[1] ISO standards, 'ISO 2685:1998', ISO. [Online]. Available: https://www.iso.org/standard/23569.html

[2] Y. Carpier, B. Vieille, M. A. Maaroufi, A. Coppalle, and F. Barbe, 'Mechanical behavior of carbon fibers polyphenylene sulfide composites exposed to radiant heat flux and constant compressive force', *Compos. Struct.*, vol. 200, pp. 1–11, Sep. 2018, doi: 10.1016/j.compstruct.2018.05.086.

[3] Y. Carpier, A. Alia, B. Vieille, and F. Barbe, 'Experiments based analysis of thermal decomposition kinetics model. Case of carbon fibers PolyPhenylene Sulfide composites', *Polym. Degrad. Stab.*, vol. 186, p. 109525, Apr. 2021, doi: 10.1016/j.polymdegradstab.2021.109525.

[4] J. Brübach, C. Pflitsch, A. Dreizler, and B. Atakan, 'On surface temperature measurements with thermographic phosphors: A review', *Prog. Energy Combust. Sci.*, vol. 39, no. 1, pp. 37–60, Feb. 2013, doi: 10.1016/j.pecs.2012.06.001.

[5] A. Chaudhary, A. Coppalle, G. Godard, P. Xavier, and B. Vieille, 'Phosphor thermometry for surface temperature measurements of composite materials during fire test', *Int. J. Heat Mass Transf.*, vol. 211, p. 124215, Sep. 2023, doi: 10.1016/j.ijheatmasstransfer.2023.124215.

[6] B. Y. Lattimer and J. Ouellette, 'Properties of composite materials for thermal analysis involving fires', *Compos. Part Appl. Sci. Manuf.*, vol. 37, no. 7, pp. 1068–1081, Jul. 2006, doi: 10.1016/j.compositesa.2005.01.029.

[7] D. Philippe, B. Vieille, and F. Barbe, 'Modelling the gradual through thickness porosity formation and swelling during the thermal aggression of thermoplastic-based laminates', *Compos. Part B Eng.*, 2023.

[8] Y. Carpier, B. Vieille, F. Barbe, and A. Coppalle, 'Meso-structure-based thermomechanical modelling of thermoplastic-based laminates subjected to combined mechanical loading and severe thermal gradients', *Compos. Part Appl. Sci. Manuf.*, vol. 162, p. 107165, Nov. 2022, doi: 10.1016/j.compositesa.2022.107165.

[9] E. Schuhler, A. Coppalle, B. Vieille, J. Yon, and Y. Carpier, 'Behaviour of aeronautical polymer composite to flame: A comparative study of thermoset-and thermoplastic-based laminate', *Polym. Degrad. Stab.*, vol. 152, pp. 105–115, 2018.

[10] B. Vieille *et al.*, 'Kerosene flame behaviour of C/PEKK composite laminates: Influence of exposure time and laminates lay-up on residual mechanical properties', *Compos. Part B Eng.*, vol. 222, p. 109046, Oct. 2021, doi: 10.1016/j.compositesb.2021.109046.

[11] E. Schuhler, A. Chaudhary, B. Vieille, and A. Coppalle, 'Fire behaviour of composite materials using kerosene burner tests at small-scales', *Fire Saf. J.*, vol. 121, p. 103290, May 2021, doi: 10.1016/j.firesaf.2021.103290.

[12] E. Schuhler, 'Dégradation des matériaux composites sous l'effet d'une flamme : application à la réaction aux feux des composites utilisés pour les transports et l'énergie', phdthesis, Normandie Université, 2019. Accessed: Apr. 22, 2024. [Online]. Available: https://theses.hal.science/tel-02926022

[13] F. P. Incropera and F. P. Incropera, Eds., *Fundamentals of heat and mass transfer*, 6th ed. Hoboken, NJ: John Wiley, 2007.